Reducing AEGIS galaxies in two filters

Sowmya Kamath, Joshua Meyers, Patricia Burchat

Abstract

This research note summarizes the procedure used to process AEGIS HST images in V and I bands to produce two-band postage stamp images of galaxies.

1 Introduction

Gravitational weak-lensing is a useful tool in cosmology and requires statistical precision and accuracy in galaxy shape measurements. The chromatic nature of the point spread function (PSF) and the varying spectral energy distribution (SED) across a galaxy profile can create additional complications in measuring the intrinsic shape of the observed galaxy. Hence to better understand chromatic effects on galaxy shapes measured by the Large Synoptic Survey telescope (LSST), it is necessary to simulate galaxy images that reflect the chromatic components of real galaxies.

We can use real galaxy images observed by HST in multiple filters to simulate real chromatic galaxies as seen by LSST, with the `ChromaticRealGalaxies` module in `GalSim` (see Github issue, pull request, and note). In this document, we describe the procedure to obtain postage-stamp images of individual galaxies from the AEGIS (All-sky Extended Groth strip International Survey) catalog in two HST filters (V and I). The method used to reduce the images is similar to that used to reduce COSMOS images in Leauthaud et al. (2007), and is an extension of work done by Bradley Emi, Rachel Mandelbaum, Andres Plaza, and Jason Rhodes in 2015 (ChromaticGalaxies Github). The final products are in a format similar to the COSMOS Real Galaxy training sample used in the third GRavitational lEnsing Accuracy Testing challenge, or GREAT3 (Mandelbaum et al., 2014). The script developed for image reduction is explained in a README file[1] and the final data products are publicly available [2]. In a separate note, we describe how we use the AEGIS galaxy images in a study of the impact of color gradients on cosmic shear measuremnts.

The work is presented as follows. In section 2 we discuss the AEGIS HST data which we use as input to create the catalog. The procedure to obtain individual galaxy images, their PSF images as well as constructing the two-band catalog is described in section 3. The final data products are described in section 4 and analyzed in section 5.

2 Input Data Set

We use unrotated ACS/WFC data, that was already reduced, to create the catalog. To model the PSF, we use star fields drawn from `Tiny Tim` software.

[1] https://github.com/GalSim-developers/GalSim/blob/%23770/devel/external/AEGIS/README.md
[2] http://great3.jb.man.ac.uk/leaderboard/data/public/AEGIS_training_sample.tar.gz

2.1 AEGIS HST data

The AEGIS HST imaging data comprises of a mosaic pattern of $21 \times 3 = 63$ contiguous HST "tiles" covering an effective area of $10.1' \times 70.5' = 710.9$ arcmin^2. Each tile was observed in a 4-pointing dither pattern in each of two filters (V and I), in order to achieve half-pixel dithering at the center of the ACS WFC, bridge the detector gap, and improve tile overlap. Detests for each of the 63 tiles consists of a science image and a weight map (Davis et al., 2007).

2.2 Science Image and Weight Map

Each reduced image has been drizzled from 4 exposures to produce final 8000×8000 pixel images with pixel sampling of $0.03''$ per pixel (Lotz et al., 2008). The dithered observations for each pointing and filter were combined ("drizzled") using MultiDrizzle. The pixel drop size was 0.8 of the input pixel size, and the final pixel size of $0.03''$ is 0.6 times the input pixel size of $0.05''$. These pixel sizes were chosen so as to reduce stochastic aliasing of the PSF (Rhodes et al., 2007). An impact of the smaller pixel scale is increased correlation in the background noise in the final drizzled image. The total exposure times and ABMAG zero-points are shown in Table 1.

Table 1: Parameters for images in V and I bands.

Filter	Total exposure time	ABMAG zero-point
F606W (V)	2260 s	26.508
F814W (I)	2100 s	25.955

The MultiDrizzle algorithm also produced inverse-variance ($1/\mathrm{RMS}^2$) weight maps for each drizzled image. The weight maps include the effects of non-uniform exposure times for the "gaps" between the ACS chips and for masked cosmic-rays. The weight maps were converted to RMS maps ($1/\sqrt{\mathrm{WEIGHT\_MAP}}$) for SExtractor measurements (see Appendix A for details on the weight map).

2.3 `Tiny Tim` Star Field

The variation in the size and ellipticity of the PSF across the focal plane of the HST ACS is dominated by the effective focus, which changes due to thermal expansion and contraction of the HST. The `Tiny Tim`[3] ray-tracing software simulates the variation of the PSF across the field for different focal lengths. The PSF variation across an image can be characterized by comparing the measured PSF ellipticity for stars in a field to the `Tiny Tim` predictions for different focus offsets, and finding the focus that best matches the measured and predicted PSFs across the field (Leauthaud et al., 2007).

[3] http://www.stsci.edu/hst/observatory/focus/TinyTim

3 Catalog Construction Procedure

The procedure we use here to create the AEGIS catalog is similar to that used for the weak lensing catalog for the HST ACS COSMOS survey (Leauthaud et al., 2007). We use version 2.8.6 of the SExtractor package to produce a source catalog of positions and various photometric parameters. The steps in the construction of the catalog and the number of objects relevant to each step are summarized in Table 2 and described in the following subsections.

Table 2: Summary of steps in construction of catalog.

Parameter	V band	I band
Raw SExtractor Detections on Co-added V+I Image		
Total number of detected objects	1.7×10^5	
Total number of faint detections	1.5×10^5	
Total number of bright detections	1.8×10^4	
Details of Cleaning Process		
Number of objects within noisy border of tile	8.9×10^3	
Number of faint detections with central pixel in bright segmentation map	2.0×10^4	
Number of objects in diffraction masks	1.6×10^3	1.6×10^3
Number of objects in manual masks	8.2×10^2	
Number of objects detected more than once in adjacent tiles	2.5×10^3	
Catalog Cleaned of Image Defects		
Total number of objects	1.3×10^5	1.3×10^5
Number of galaxies	1.3×10^5	1.3×10^5
Number of stars	1.3×10^3	1.8×10^3
Catalog with $\mathrm{F814W}_{\mathrm{ABmag}} < 25.2$		
Total number of galaxies	2.9×10^4	
Final Catalog after removing bad postage stamps		
Total number of galaxies	2.7×10^4	

3.1 Detection in Co-added Images

We use SExtractor in the dual-image mode; detecting objects with the summed V+I images and then performing photometry on the individual V and I images at those detected locations. This ensures that the catalogs have the same objects in both bands.

The input RMS map corresponding to the co-added image was created by taking the reciprocal of the weight maps in both bands, adding them and then taking the square root of the content of each pixel.

3.2 "Hot-Cold" Detection Method

To construct a catalog of objects useful for weak-lensing studies, we must be efficient in detecting the small faint objects that contain much of the lensing signal. We therefore configure SExtractor with very low detection thresholds (even if this leads to false detections) and apply selection criteria to clean the catalog later. However, when configured with low detection thresholds, SExtractor inevitably shreds low surface brightness spirals

and patchy irregulars, detects spurious objects in the scattered light around bright objects, while failing to separate overlapping pairs of objects. To remedy these problems we adopt the method used by Leauthaud et al. (2007), which was an improvement upon the "Hot-Cold" method used in the GEMS survey data analysis (Rix et al., 2004). We run SExtractor twice, once with a configuration optimized for the detection of only the brightest objects ("cold"), and then again with a configuration optimized for the faint objects ("hot" step). The higher detection threshold of the bright step improves the detection of close pairs. Masks are created to remove false detections around bright objects, and then the two samples are merged to form the final catalog.

The Sextractor configuration parameters used for the detection of bright and faint objects are shown in Table 3. All other parameters are set to their default values. We will refer to the resultant catalogs of detected objects as C_{bright} and C_{faint}. The segmentation maps created in each step are saved, to be used later when the two catalogs need to be merged, as well as in creating a combined segmentation map.

Table 3: SExtractor configuration parameters for bright and faint object detection.

Parameter	Bright Objects	Faint Objects
DETECT_MINAREA	140	18
DETECT_THRESH	2.2	1.0
DEBLEND_NTHRESH	64	64
DEBLEND_MINCONT	0.04	0.065
CLEAN_PARAM	1.0	1.0
BACK_SIZE	400	100
BACK_FILTERSIZE	5	3
BACKPHOTO_TYPE	Local	Local
BACKPHOTO_THICK	200	200

3.3 Merging Bright and Faint Catalogs

To remove spurious detections around bright objects, the region associated with each object in the segmentation map of the bright object is extended by 15 pixels in all directions[4]. Objects in the faint catalog (C_{faint}) are then removed if their centroid lies within an extended region associated with a bright object. The final catalog is obtained by merging *all* objects in the bright catalog (C_{bright}) with the remaining faint objects.

3.4 Cleaning the catalog

Care is taken to remove unreliable regions of images and false detections. The following regions were masked and objects detected within the regions were excluded from the final catalog.

[4]For the COSMOS catalog in Leauthaud et al. (2007), a 20-pixel buffer was used around bright objects. We found that the narrower buffer remedied problems in a later step where we combine segmentation maps; see subsection 3.7.

- **Image boundaries**: Each ACS/WFC pointing consists of four slightly offset, dithered exposures, making detection less reliable near the boundaries of each tile where there are fewer than four input exposures. Because adjacent tiles overlap sufficiently, we are able to eliminate these regions near the boundaries without reducing the number of detected objects. Objects are included in the catalog only if their centroid lies within the area demarcated by the green box shown in the image on the right of Figure 1. The same area is used for all tiles and for both filters.

- **Diffraction spikes**: Objects near bright stars or saturated pixels were masked to avoid shape biases due to any background gradient. Stars with magnitude less than 19 are taken to be saturated. An automatic algorithm was developed to define polygonal-shaped masks around saturated stars, with a size scaled by the FLUX_AUTO of the star. The diffraction spike mask for a saturated star is shown as the yellow polygon in the image on the right in Figure 1. The width of the spike mask was set to 40 pixels. The length of the spike mask was determined from a linear fit to FLUX_AUTO versus the length of the spike measured manually, for 10 saturated stars. The angle was set to the mean of the angles by which the manually measured spikes were found to be rotated relative to the x-y axes. The parameters defining the mask were computed separately for each filter.

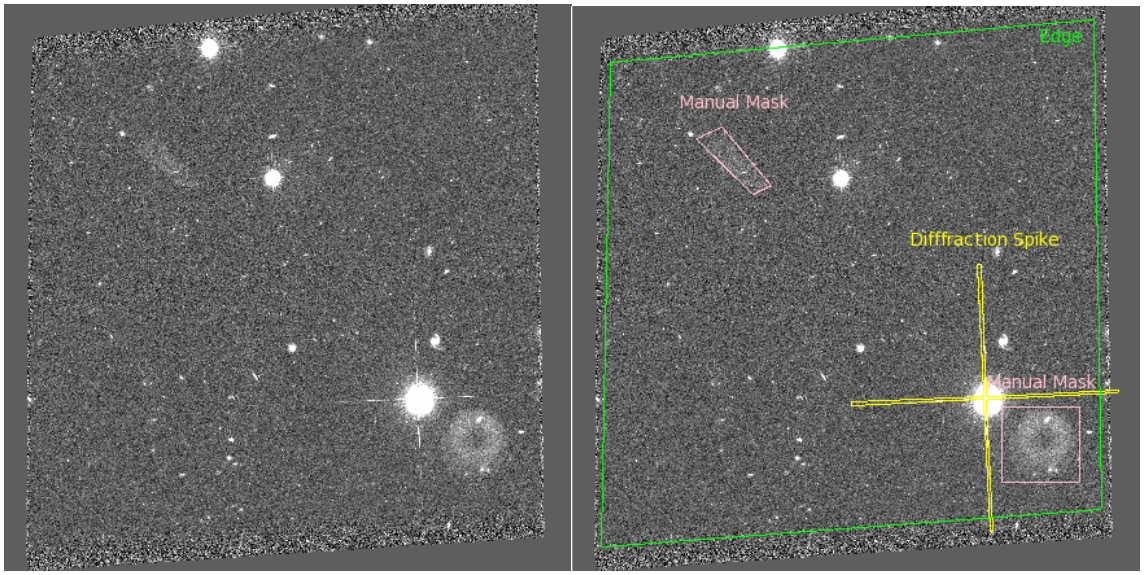

(a) Raw image.

(b) Boundary edge (green), automated diffraction spike mask (yellow), and manual mask (pink).

Figure 1: (a) Raw image. (b) Examples of masking.

- **Manual masks**: In a few cases where the automatic diffraction-spike masking algorithm failed, the masks were created by hand. Other artifacts or contaminated regions were also masked, including "ghosts" due to internal reflections. The pink boxes in the image on the right in Figure 1 show two such regions that were discovered upon visual inspection and manually masked.

- **Multiple detections**: Pairs of objects whose centroids are within 2 arcseconds

of each other (typically due to the overlap between adjacent tiles) were marked as multiple detections. The object with the highest value of SExtractor FLAG (indicating a poor detection) was discarded. If the multiple detections have the same FLAG, the object with higher SNR was kept.

This gives a catalog of around 1.3×10^5 unique detections (see Table 2).

3.5 Star-Galaxy Separation

Since the goal here is to obtain a sample of **galaxy** images in multiple bands, star-galaxy separation is important. Also, a clean sample of stars is important for modeling the PSF. The CLASS_STAR parameter of SExtractor is unreliable since it was trained with ground-based images and is therefore only valid for a sample of profiles similar to the original training set (Leauthaud et al., 2007). Therefore, we use an alternate method that was used in the COSMOS catalog construction to classify point sources and galaxies, based on the SExtractor parameters MU_MAX (peak surface brightness above the background level) and MAG_AUTO. Since the surface brightness of a point source scales with magnitude, and that of extended objects does not, stars occupy a well-defined locus in a plot of MU_MAX vs. MAG_AUTO, whereas galaxies do not. The criteria used to classify stars and galaxies is illustrated by the black line in the plot for each filter in Figure 2. Since point sources are difficult to separate from small faint galaxies, we only use star candidates with magnitudes less than 25. In the figure, the red dots denote star candidates and the blue dots show the galaxy candidates. The yellow circles denote stars that were selected for PSF estimation as described below.

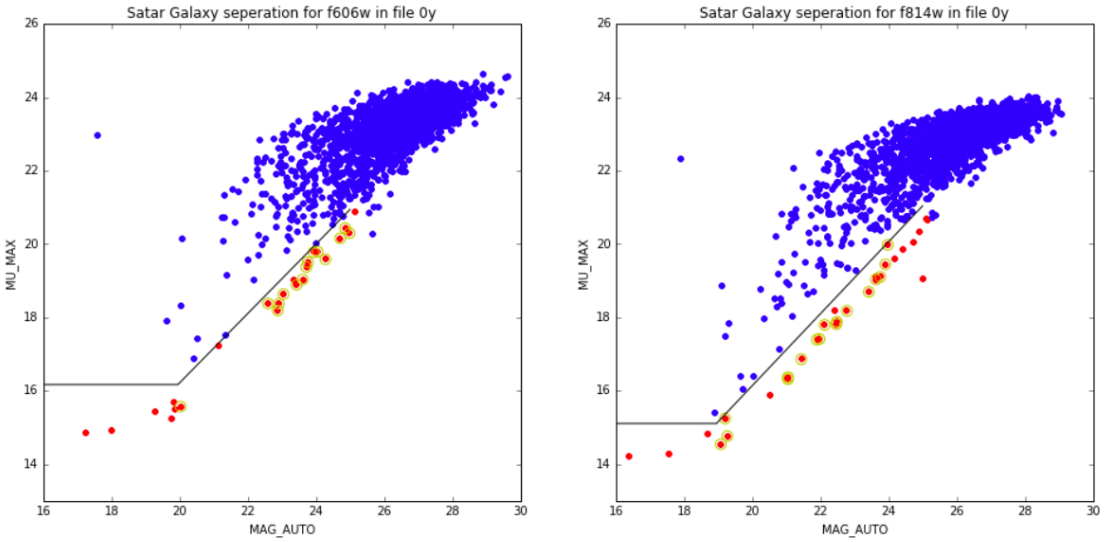

Figure 2: Star-galaxy separation in a plot of peak surface brightness vs. magnitude, for V band (left) and I band (right) for sources in a single tile. The black line shows the line used to separate stars and galaxies. The red dots denote star candidates while the blue dots denote galaxy candidates. Stars with yellow circles are selected for PSF estimation.

3.6 PSF Estimation

Although the ACS/WFC PSF is not stable, most of the PSF variation can be ascribed to a single physical parameter. Thermal expansions and contractions of HST alter the distance between the primary and secondary mirrors. As the effective focus deviates from nominal, the PSF becomes larger and more elliptical, with the direction of elongation depending on the position above or below nominal focus (Rhodes et al., 2007). The `Tiny Tim` ray-tracing program is used to create a grid of model PSF images at varying focus offsets. By comparing the ellipticity of ≈ 15 stars in each image to the `Tiny Tim` predictions at those locations, we determine the image's effective focus.

Up-to-25 stars with the highest SNR were selected for PSF estimation in each tile. The "star" in the `Tiny Tim` model closest to each of the above stars was identified. Only star candidates that were 1) not masked, 2) had no other object close to them, 3) had a `Tiny Tim` star within 200 pixels, and 4) were classified as stars in both bands were selected for PSF estimation. A cost function was defined as the sum of the squares of the differences in each ellipticity component for the real and simulated stars, where the ellipticity is defined in terms of the second moments. The focus offset was chosen as that corresponding to the lowest cost function. A sample plot of cost function versus focus offset is shown in Figure 3. The vertical dashed line shows the value of focus offset.

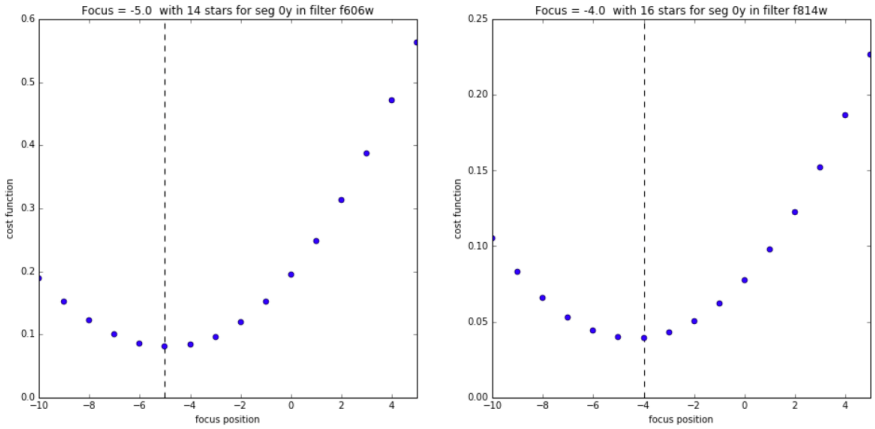

Figure 3: Cost function for different values of focus offset for V band (left) and I band (right). The vertical dashed line shows the selected focus offset value.

For each image, the focus offset was calculated for all stars that passed the criteria described above, and then recalculated dropping the lowest SNR star. This was repeated until only 3 stars were left. Figure 4 shows the focus offset corresponding to the minimum value of the cost function for different numbers of stars used to compute the cost function, in a single sample image. The modal value of focus offset was selected for each image, illustrated as the horizontal dashed line in the plot.

3.7 Combined Segmentation Map

Our main objective is to obtain **individual** galaxy images in multiple bands – i.e. individual postage stamps of galaxies. If there are more than one galaxies in a postage stamp, the cleaning step masks the non-central galaxies with noise. However postage stamps where

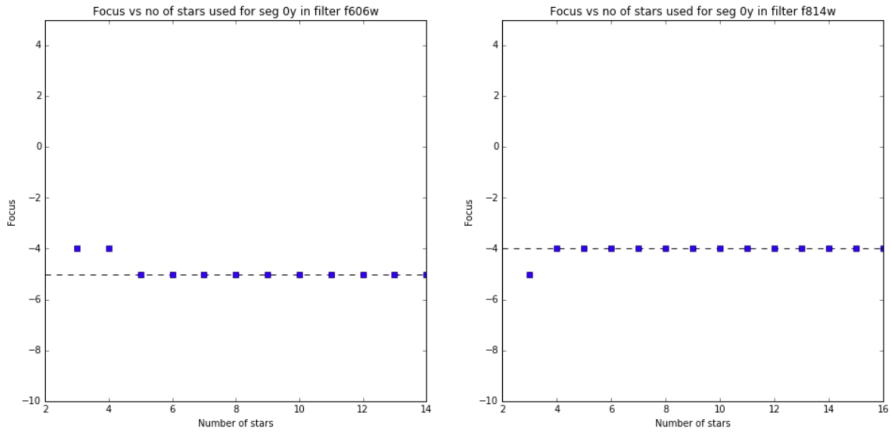

Figure 4: Focus offset corresponding to minimum cost function for different numbers of stars used to calculate the cost function for V band (left) and I band (right). The horizontal dashed line shows the focus offset selected.

the masked object is too close to the central object, or where the masking was insufficient, are identified and eliminated in the selection step. Identifying these multiple galaxies is done with a segmentation map that includes all regions corresponding to objects in the bright-faint merged catalog, hereafter called the combined segmentation map. Since we care more about obtaining a pure sample than a complete sample, the cleaning step has been made stringent. Eliminating a few good galaxies in the selection step is preferable to having postage stamps with multiple objects that cannot be cleaned. Several factors are considered in making the combined segmentation map:

1. Each object in the catalog must correspond to only one region.
2. The detection limits and hence segmentation maps for bright and faint detections will be different.
3. The combined map must not shred objects.
4. Close-by objects should be identified as different regions.

Bright/faint objects in the combined segmentation map will have a region corresponding to their region in the bright/faint segmentation map. If a pixel was detected to belong to different objects in the bright and faint step, it is assigned to the bright object in the segmentation map. The original segmentation region corresponding to any object in the bright catalog is expanded by 5 pixels. This is done because detection limits were set much higher for the bright objects and the segmentation maps obtained thus do not encompass the whole object.

As noted earlier (subsection 3.3), in the COSMOS reduction procedure objects in the faint catalog are added to the merged catalog only if the center of the faint object does not lie inside the bright segmentation buffered by 20 pixels. However, a small faint object that lies within this buffered region will not be included in the merged catalog as well as in the combined segmentation map, leading to it not being replaced by noise in the cleaning step. To reduce such occurrences we decided to reduce the buffer size from 20 to 15 pixels.

3.8 Galaxy Selection

The following criteria are used to select objects for the final galaxy catalog:

- The object is not classified as a star in either filter.
- The object is not in a masked region in either filter.
- The object has SNR > 0 in both filters.
- Object has MAG_AUTO less than 25.2 in the I (F814W) band.

28,532 objects that satisfy the above criteria (see Table 2) are then used to make the postage stamps.

3.9 Galaxy Postage Stamps

Rectangular postage stamps are made for each selected galaxy. The size of the postage stamp for each galaxy is determined using equations 2 and 3 in Haussler et al. (2007):

$$\text{XSIZE} = 2.5\, a\, \text{kron} \Big(|\sin\theta| + (1 - \text{ellip}) |\cos\theta| \Big), \tag{1}$$

$$\text{YSIZE} = 2.5\, a\, \text{kron} \Big(|\cos\theta| + (1 - \text{ellip}) |\sin\theta| \Big), \tag{2}$$

where a is the SExtractor output parameter A_IMAGE, kron is KRON_RADIUS, θ is THETA_IMAGE, and ellip is ELLIPTICITY. The parameters XSIZE and YSIZE are individually computed for each filter and the highest value sets that dimension of the postage stamp for both filters. Postage stamps with the same dimensions are also drawn for the combined segmentation map and used in the cleaning step below.

3.10 Cleaning Postage Stamps

In crowded regions, the galaxy postage stamps may contain other neighboring objects. These contaminating galaxies will influence shape measurements of the central galaxy and hence have to be removed. We ensure that there is only one galaxy per postage stamp by replacing the pixel content for the other objects with noise.

The combined segmentation map of the region is used to determine which pixels correspond to the central galaxy, which to the contaminating galaxies, and which are background. Pixels that correspond to any object except the central object in the galaxy postage stamp are replaced with noise. The noise is drawn from a noise map created for each filter, described in subsection 3.12 below. Thus each postage stamp has only the central galaxy image.

3.11 Identifying Bad Postage Stamps

After the above cleaning postage stamp step, we find that sometimes the other object was too close to the central galaxy or too bright for it to be effectively masked. If a galaxy is too bright, then its segmentation region (computed with bright SExtractor settings) is not able to encapsulate all the bright pixels, leading to imperfect masking. Also since the segmentation map assigns a pixel to only one galaxy if two galaxies are very close to

each other, pixels shared by both will be assigned to one or the other. This may result in abrupt changes in the assignment of neighboring pixels, causing sharp edges in the surface brightness profiles in the cleaned galaxy postage stamps. Also postage stamp cleaning step does not take into account overlapping galaxies that were identified as a single object in the detection step, leading to spurious galaxy shapes.

We use the technique employed in Mandelbaum et al. (2014) to help identify such bad postage stamps. During the cleaning step we identify the pixel that is closest to the center of the postage stamp (i.e., the center of the selected object) *and* whose was replaced by noise. Two values are measured for this pixel separately in each band:

1. `min_mask_dist_pixels`: the distance from the center of the postage stamp to the closest replaced pixel;

2. `average_mask_adjacent_pixel_count`: the average flux in the 3×3 pixel region around this closest replaced pixel, before replacing with noise.

A "bad stamp" flag is set if any of the following conditions true:

1. `HSM` module of `GalSim` was not able to compute moments and the SExtractor parameter ELLIPTICITY ≤ 0.75, in any filter.

2. `min_mask_dist_pixels` ≤ 5.

3. $5 <$ `min_mask_dist_pixels` ≤ 11 pixels *and* `average_mask_adjacent_pixel_count` is greater than 20% of the brightest pixel in the stamp.

Galaxies with the bad stamp flag in any filter are removed from the final catalog. We are left with 26,517 good galaxy postage stamps in our final catalog, for both bands.

3.12 Creating the Noise Map

The drizzling process introduces correlations between neighboring pixels, which artificially reduces the noise level of co-added drizzled images. Care is taken to preserve these correlations when generating noise maps to replace pixel values for nearby objects.

Sixteen empty regions of varying sizes, with dimensions ranging from 70-700 pixels, at different positions on the image plane, were visually identified. A 50×50 covariance matrix for the pixel values was calculated for each empty region (separately in each filter) and their mean computed, as shown in Figure 5. Noise maps generated from the mean covariance matrix for each filter are shown in Figure 6.

To replace nearby objects with noise, a region that is identical in size and shape to the nearby object in the segmentation map is cut from a random location in the noise map shown in Figure 6 and used to replace the pixel values of the nearby object in the galaxy postage stamp.

3.13 Parametric Fits

The COSMOS catalog galaxies for the GREAT3 challenge were subject to an additional step of fitting for parametric models. This step was not performed here, and the values in the output catalogs corresponding to these parameters were arbitrarily set to 999.

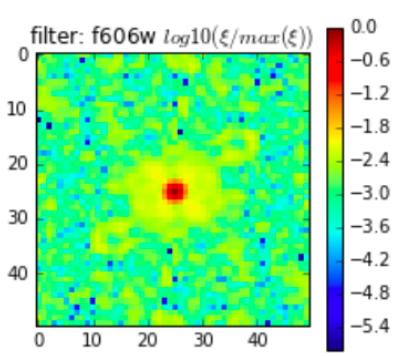

(a) Covariance map in V (F606W) filter.

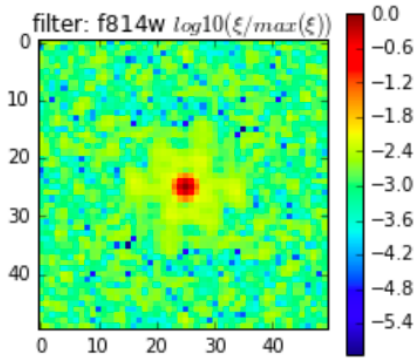

(b) Covariance map in I (F814W) filter.

Figure 5: Mean co-variance matrix in the two filters.

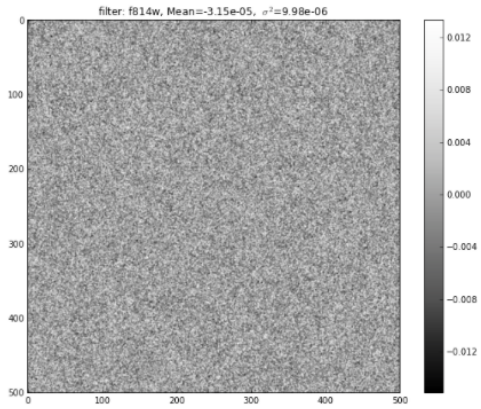

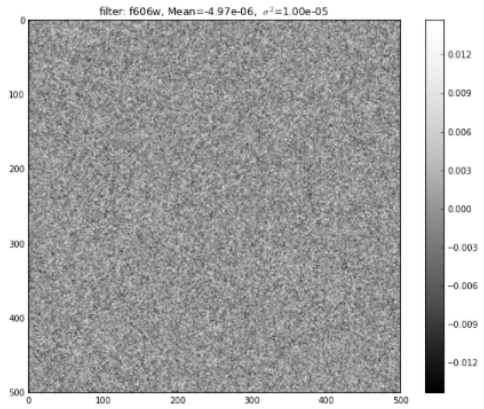

Figure 6: Image of noise map generated from covariance matrices, for I band (left) and V band (right).

3.14 PSF Postage Stamps

The PSF for each galaxy is taken to be the `Tiny Tim` model PSF image whose location in the `Tiny Tim` grid is closest to that galaxy's position in the focal plane, for the best-fit focus offset as described in subsection 3.6. Square postage stamps (20×20 pixels) are drawn for each filter.

3.15 Additional Catalogs

The Extended Groth Strip (EGS) has been extensively studied with other surveys in other bands. We include in our catalog photometry and spectroscopic redshift measurements from other catalogs, for objects in our catalog with a center within 1 arcsecond of an object in the other catalog.

We also include in our final catalog the spectroscopic redshifts for 3763 matched galaxies from the DEEP2 galaxy redshift survey, Data Release 4 (Newman et al., 2012). The redshift distribution for these matched galaxies is shown in Figure 7.

We also include in our catalog the results from the photometry catalog of the AEGIS field (Lotz et al., 2008). We compare in Figure 8 the magnitude we measure with SExtractor to the magnitude in the AEGIS photometry catalog for 27,289 matched objects.

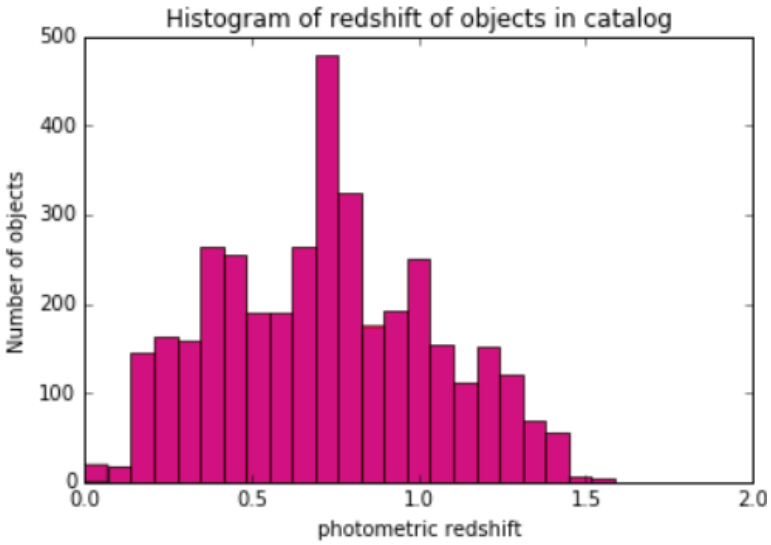

Figure 7: Spectroscopic redshifts for selected galaxies that also appear in the DEEP2 redshift survey.

The magnitudes of bright objects in the two catalogs are in good agreement. However for larger magnitudes, there are a few objects that were measured to be fainter in the AEGIS photometric catalog than in this catalog.

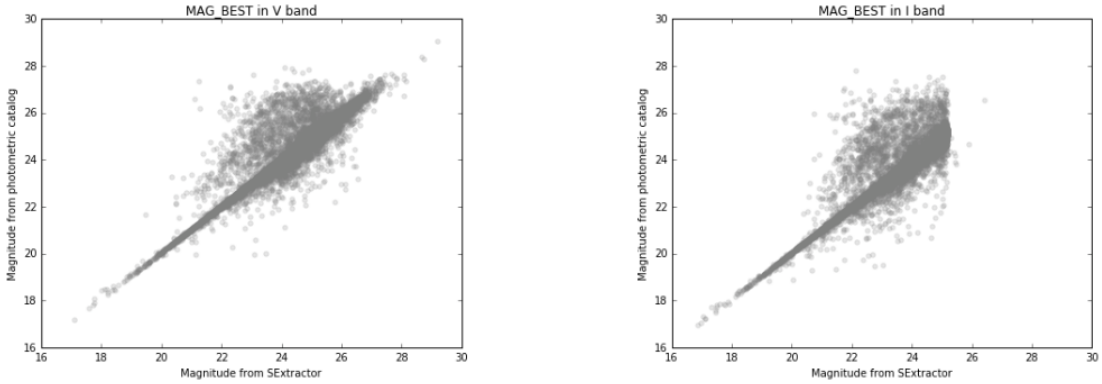

Figure 8: Magnitudes in AEGIS catalog plotted versus magnitudes calculated with SExtractor for this study.

4 Data Products

The output files are in the format expected by `galsim.RealGalaxyCatalog`. The format of the output files and the saved attributes are explained in detail in the AEGIS catalog README file. For each band, the output files are:

1. Main catalog (hereafter referred to as the GalSim catalog);
2. Files with postage stamp images of galaxies;
3. Files with postage stamp images of PSF;
4. Catalog with information on parametric fits (step not performed here);

5. Catalog with information for selection cuts;

6. File with noise correlation function.

The GalSim catalogs contain only select details about the galaxies. A complete catalog with more columns is also created, which has all the columns in the GalSim catalog along with the parametric fits catalog, selection catalog, information from additional catalogs, and other measured values from SExtractor.

5 Object Characteristics

In Figure 9, we show the distribution of magnitudes computed by SExtractor in V and I band, and V−I color, as well as a color-magnitude plot, for the 26,517 objects in the final catalog. Recall from subsection 3.8 that a magnitude cut of 25.2 was made in the I band only.

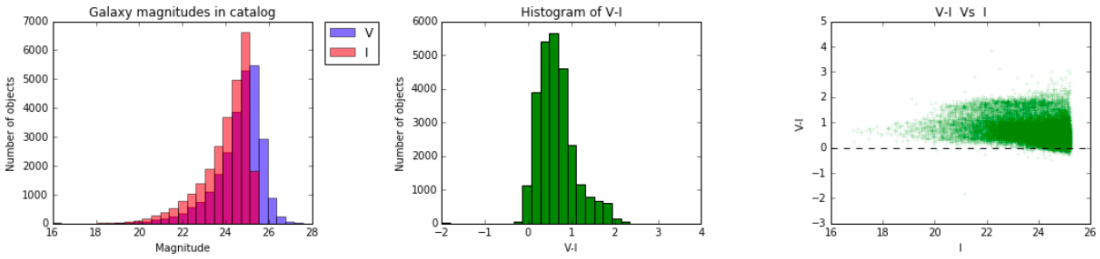

Figure 9: Distributions for the 29,105 selected objects. a) Magnitude in V band and I band. b) Difference in magnitudes (V−I color). c) V−I color vs. I band magnitude.

In Figure 10, we show the SNR distribution in each band for the selected galaxies. The SNR was measured with an elliptical Gaussian filter matched to the galaxy profile with the `HSM` module of `GalSim`. This SNR calculation does not take into account the fact that the noise is correlated between pixels; hence the noise is under-estimated. The corrected SNR would be approximately half the values plotted here (see section 3.8 in Leauthaud et al. (2007)).

In Figure 11, postage stamps are shown for the galaxy images (left) and the corresponding `Tiny Tim` PSF images (right) for V band (top) and I band (bottom), for a sample galaxy. As noted in earlier sections, the size of the rectangular galaxy postage stamp is matched to the galaxy size and is the same in both filters, while the PSF postage stamps are always 20 pixel × 20 pixel squares.

5.1 Selection Effects and Weight Function

The process of picking galaxies for the final catalogs can introduce certain unwanted selection effects. Selection effects become evident when the galaxies that pass the selection cuts to be included in the final catalog (2.7×10^4 galaxies in Table 2, hereafter final catalog) are compared to the galaxies in the catalog of galaxies with $\mathrm{F814W_{AB}} < 25.2$ (2.9×10^4 galaxies in Table 2, hereafter parent catalog). Figure 12 shows the fraction of galaxies from the parent catalog that are included in the final catalog as a function of four parameters

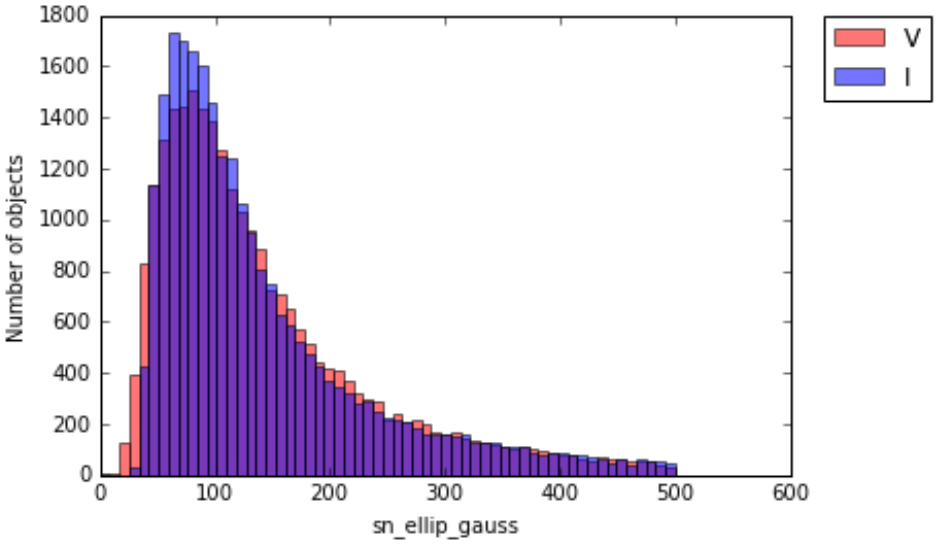

Figure 10: Distribution of the galaxy flux SNR, measured with an elliptical Gaussian filter.

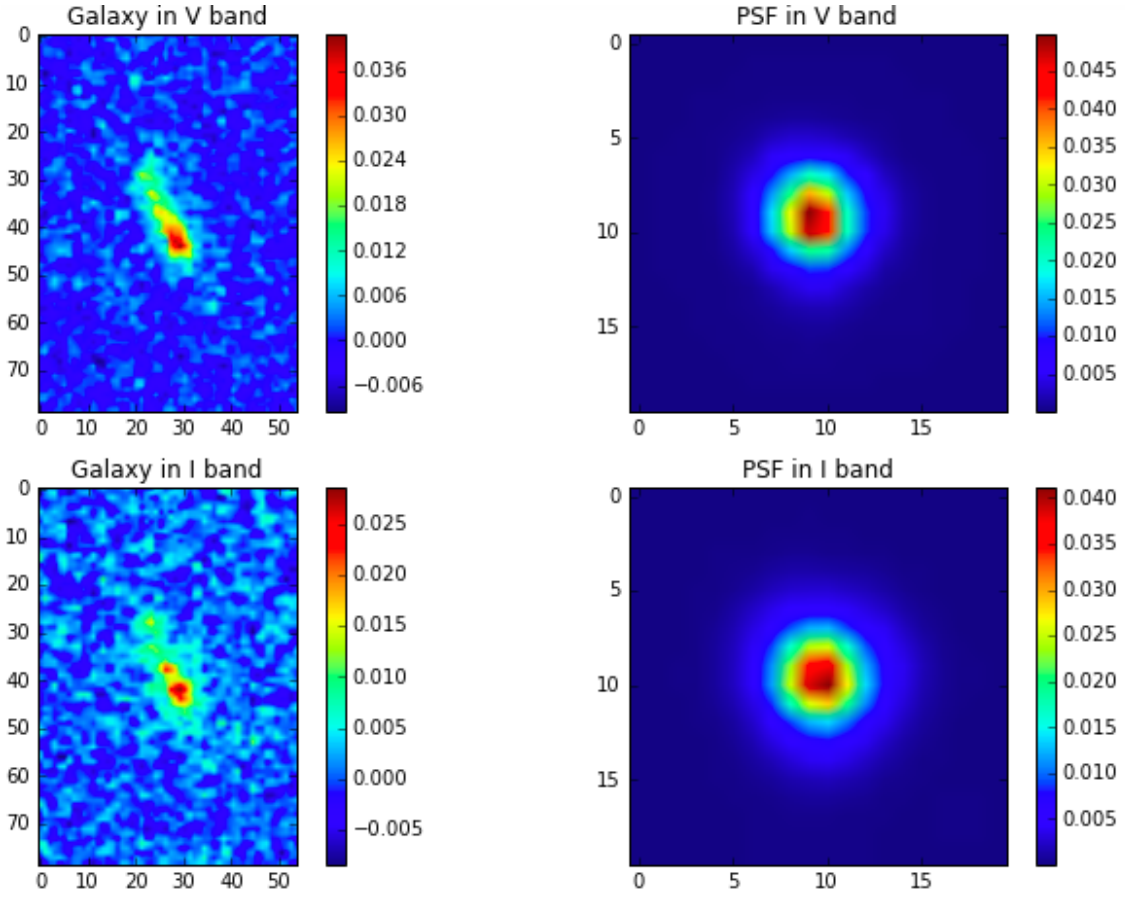

Figure 11: Postage stamps for the galaxy images (left) and the corresponding `Tiny Tim` PSF images (right) for V band (top) and I band (bottom), for a sample galaxy.

estimated by SExtractor: `FLUX_RADIUS` (half-light radius), `ELLIPTICITY` (magnitude of ellipticity, $1 - b/a$), `THETA_IMAGE` (position angle) and `MAG_AUTO` (AB magnitude). We can see a clear dependence of the fraction on the size of the galaxy, while the other parameters don't seem to influence it.

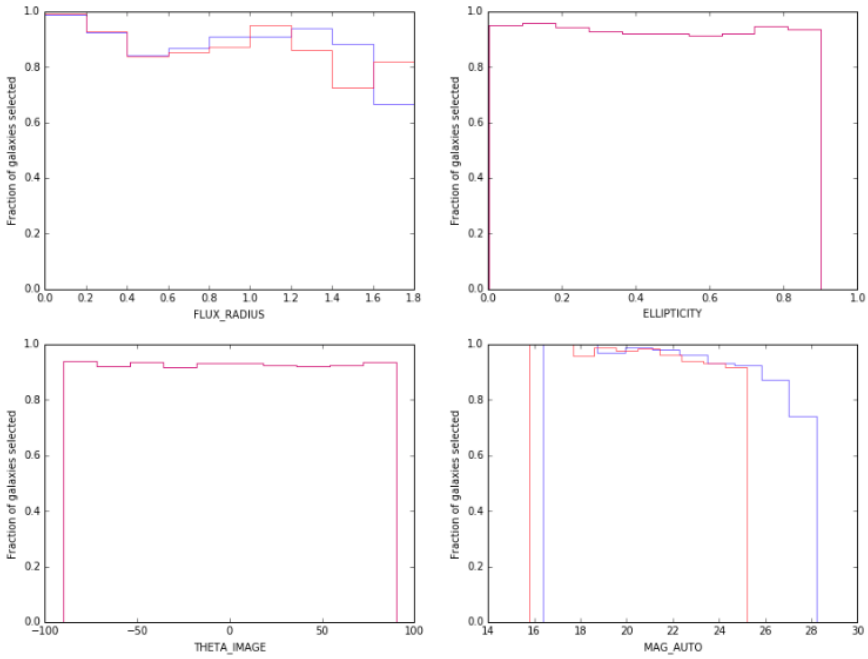

Figure 12: Histogram of fraction of galaxies selected in the final catalog as a function of half-light radius, ellipticity, position angle, and magnitude in I band (red) and V band (blue).

A drop in the fraction of selected galaxies for large galaxies is primarily due to them being shredded during the detection, causing them to be improperly masked in the postage stamp cleaning step, leading to failed moments measurement and failing the selection cuts.

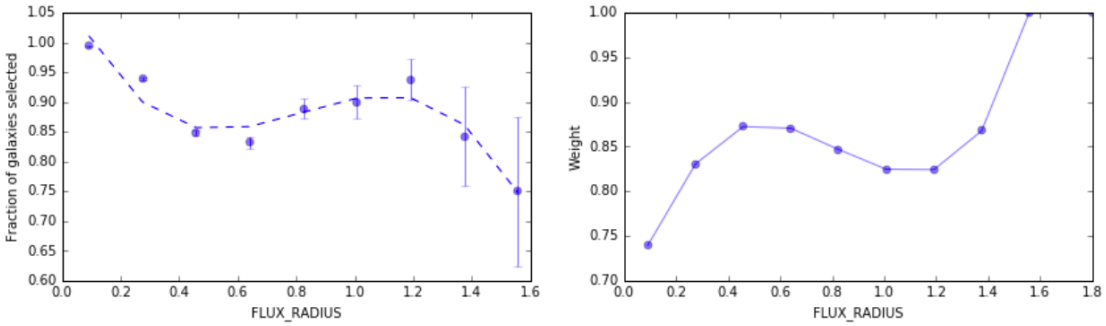

Figure 13: Left: Fraction of galaxies selected in the final catalog as a function of half-light-radius (solid dots) along with the fitted curve (dashed line). Right: Weights computed for different half-light-radii. The weight is defined such that large galaxies have value 1.

To account for this selection effect, we assign a size-dependent weight to every galaxy. Since the magnitude cut was applied only to the I band, the weight is computed only in this band. Thus galaxies in both bands have the same `WEIGHT`, computed based on its I-band size. The weight is defined as the reciprocal of the fraction of galaxies that passed the selection cuts, normalized to 1 for large galaxies. The left panel of Figure 13 shows the fraction as a function of half-light radius (solid points). A curve is fit through the points (dashed line) and used to compute the weight for different galaxy sizes. The right panel shows the computed weight as a function of half-light-radius.

6 Future Work

This work was done with the goal of obtaining real galaxy images in the two AEGIS HST bands to produce realistic chromatic galaxy images as would be seen by other surveys. However, the pipeline can be used to reduce any HST images in multiple bands – e.g., the CANDELS survey. Parametric fits can be performed on the galaxies and studied. The images can also be used for the analysis of multi-band galaxy fits.

References

Davis, M., Guhathakurta, P., Konidaris, N. P., et al. 2007, Astrophys. J., 660, L1

Haussler, B., McIntosh, D. H., Barden, M., et al. 2007, Astrophys. J. Suppl. Ser., 172, 615

Leauthaud, A., Massey, R., Kneib, J.-P., et al. 2007, Astrophys. J. Suppl. Ser., 172, 219

Lotz, J. M., Davis, M., Faber, S. M., et al. 2008, Astrophys. J., 672, 177

Mandelbaum, R., Rowe, B., Bosch, J., et al. 2014, Astrophys. Journal, Suppl. Ser., 212, arXiv:1308.4982

Newman, J. A., Cooper, M. C., Davis, M., et al. 2012, Astrophys. J. Suppl. Ser., 208, 5

Rhodes, J. D., Massey, R. J., Albert, J., et al. 2007, Astrophys. J. Suppl. Ser., 172, 203

Rix, H.-W., Barden, M., Beckwith, S. V. W., et al. 2004, Astrophys. J. Suppl. Ser., 152, 163

Appendix A Weight Maps as Input to SExtractor

SExtractor handles images with variable noise through weight maps, which describe the expected noise level at each pixel. These maps are internally stored in units of absolute variance (in ADU^2). Several types of weight maps can be input to SExtractor, which converts the map to its internal variance format, controlled through the WEIGHT_TYPE configuration keyword. If a variance map is given as input – i.e., WEIGHT_TYPE is MAP_VAR – then the input file is assumed to contain a weight map in units of *relative* variance. A robust scaling to the appropriate *absolute* variance is then performed by comparing this variance map to an internal, low-resolution, absolute variance map built from the science image itself. If WEIGHT_TYPE is MAP_WEIGHT, then the specified FITS image must contain a weight map in units of relative weights (proportional to the inverse of the variance). The data is converted to variance units ($\propto$ 1/weight) and scaled as for MAP_VAR. Finally, if WEIGHT_TYPE is MAP_RMS, then the input map must be in units of absolute standard deviations (in ADUs per pixel). (See Section 8 in the SExtractor manual for details.)

The AEGIS weight map produced during the co-adding the dithered images with MultiDrizzle is produced with weight type MAP_WEIGHT, but in *absolute* units. Since SExtractor assumes MAP_WEIGHT (and MAP_VAR) weight types to be in *relative units*, we save the square root of the reciprocal of each weight map pixel in a new weight map and set the weight type to MAP_RMS so that no normalization is performed by SExtractor.